Experimental And Topological Determination of the Pressure-Temperature Phase Diagram of Racemic Etifoxine, a Pharmaceutical Ingredient with Anxyolitic Properties

M. Barrio, H. Allouchi, J.-Ll Tamarit, R. Céolin, L Berthon-Cédille, Ivo B. Rietveld

EXPERIMENTAL AND TOPOLOGICAL DETERMINATION OF THE PRESSURE-TEMPERATURE PHASE DIAGRAM OF RACEMIC ETIFOXINE, A PHARMACEUTICAL INGREDIENT WITH ANXIOLYTIC PROPERTIES

M. Barrio[1], H. Allouchi[2], J.-Ll. Tamarit[1], R. Ceolin[1,3], L. Berthon-Cédille[4], I.B. Rietveld[5,6,*]

[1] Grup de Caracterització de Materials, Departament de Física and Barcelona Research Center in Multiscale Science and Engineering, Universitat Politècnica de Catalunya, EEBE, Campus Diagonal-Besòs, Av. Eduard Maristany 10-14, 08019 Barcelona, Catalunya, Spain

[2] EA SIMBA: Synthèse et Isolement de Molécules BioActives, Laboratoire de Chimie Physique, Faculté de Pharmacie, 31, avenue Monge - 37200 Tours, France

[3] LETIAM, EA7357, IUT Orsay, Université Paris Sud, rue Noetzlin, 91405 Orsay Cedex, France

[4] Biocodex, Centre de Recherche, ZAC de Mercière, Chemin d'Armancourt, 60200 Compiègne, France

[5] Normandie Université, Laboratoire SMS - EA 3233, Université de Rouen, F 76821 Mont Saint Aignan, France

[6] Faculté de Pharmacie, Université Paris Descartes, USPC, 4 avenue de l'observatoire, 75006, Paris, France

* Corresponding author : ivo.rietveld@univ-rouen.fr

ABSTRACT

Information about the solid-state properties of etifoxine has been lacking, even if the active pharmaceutical ingredient has been used for its anxiolytic properties for decennia. The crystal structure of the racemic compound possesses a monoclinic space group P2$_1$/n with cell parameters a = 8.489(2) Å, b = 17.674(2) Å, c = 20.883(3) Å, β = 98.860(10)° and a unit-cell volume of 3095.8(9) Å^3 at 293 K. The unit cell contains 8 molecules, while 2 independent molecules with different conformations are present in the asymmetric unit. The density of the crystal is 1.291 g/cm^3 and its melting point was found at 362.6 ±0.3 K with a melting enthalpy of 85.6 ±3.0 J g^{-1}. Its thermal expansion in the liquid and the solid state and the change in volume on melting and between the vitreous state and the crystalline solid have been studied. The results confirm the tendency of small organic molecules to increase about 11% in volume on melting, while the volume difference between the glass and the crystal at the glass transition temperature is about half this value at 6%. These values can be used in the construction of phase diagrams in the case that the experimental data for a given system is incomplete.

Keywords: active pharmaceutical ingredient, thermodynamic properties, crystallographic properties, solid state, phase diagram, melting, vitreous state

INTRODUCTION

The active pharmaceutical ingredient (API) etifoxine (**Figure 1**) was developed about 60 years ago and the racemic compound is marketed for its anxiolytic properties.[1-3] Its anxiolytic effect is comparable with that of some benzodiazepine drugs such as lorazepam, but it has less side effects.[2, 4, 5] Etifoxine is prescribed in France and in some other countries, considering this drug as a safe alternative to benzodiazepine drugs. Although it has been marketed for years, structural and thermodynamic solid-state studies remain inadequate, even if its unit cell has previously been published in the CSD.[6, 7] The main purpose of the present study was to provide this data and the results are presented hereafter.
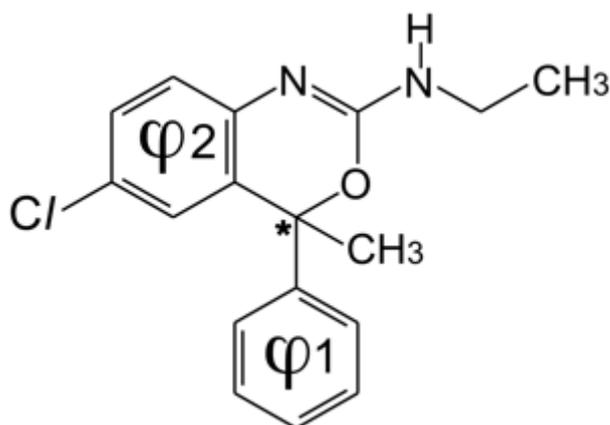

Figure 1. Chemical formula of racemic etifoxine. C$_{17}$H$_{17}$ClN$_2$O, M = 300.786 g mol^{-1}. IUPAC name: 6-chloro-N-ethyl-4-methyl-4-phenyl-3,1-benzoxazin-2-amine. The stereogenic center is indicated by an asterisk.

Besides the API-specific use of the properties determined in this paper, the data also contribute to statistical information that can be used to study the general solid-state behavior of small organic molecules, which make up a large part of the present-day marketed oral drugs. In this light, the thermal expansion of the solid and of the liquid of etifoxine will be compared to that of other APIs. Moreover, the experimental thermal expansion will be used to determine the change in volume of the compound on melting and the difference in volume between the crystalline solid and the vitreous state. This kind of data appears to be relatively constant among small organic molecules and that knowledge is important because the data can therefore be used to construct phase diagrams of APIs such as volume-against-temperature representative of the Helmholtz free energy and the better-known pressure-against-temperature representative of the Gibbs free

energy. Thus, even if very little is known about the specific volume of a given API, because it has not been determined or cannot be determined due to decomposition, it will still be possible to determine its phase behavior and with it the stability hierarchy between different solid phases of an API.

MATERIALS AND METHODS

ETIFOXINE SAMPLE

A sample of racemic etifoxine powder of medicinal grade (D4223) was kindly provided by Biocodex, France. It was used as such, while for single crystal X-ray diffraction studies suitable crystals were obtained by slow evaporation from *n*-hexane solutions at room temperature (see **Figure 2**).
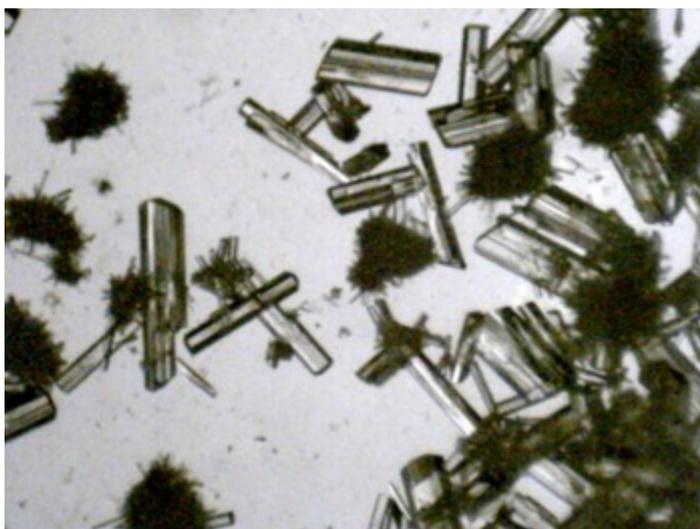

Figure 2. Optical microscopy photograph of single crystals of racemic etifoxine, obtained by slow evaporation of a solution in *n*-hexane at room temperature. The biggest crystals measure 1 to 3 mm in length.

SINGLE CRYSTAL X-RAY DIFFRACTION.

X-ray diffraction intensities were collected at room temperature up to $\theta = 65°$ (θ_{max}) with an Enraf-Nonius CAD4 diffractometer using Cu-$K\alpha$ radiation ($\lambda = 1.54178$ Å) and equipped with a graphite monochromator.[8] Unit cell determination, data collection, and data reduction were carried out with the CAD4 Express Enraf-Nonius programs package and XCAD4.[9] All data were corrected for Lorentz polarization effects. The structure was solved by direct methods using the SHELXS-97 package with which most non-hydrogen atoms were located.[10, 11] The remaining atoms were located after successive Fourier synthesis runs. The atomic parameters were refined by a least-squares method on F^2 with SHELXL-97.[10, 11] The coordinates of all non-hydrogen atoms were refined with anisotropic thermal parameters. Hydrogen atoms were placed at calculated positions generated according to stereochemistry and refined using a riding model in SHELXL-97.

HIGH-RESOLUTION POWDER X-RAY DIFFRACTION

PXRD measurements were performed with a vertically mounted INEL cylindrical position-sensitive detector (CPS-120) using the Debye–Scherrer geometry and transmission mode. Monochromatic Cu-Kα_1 (λ = 1.54056 Å) radiation was selected by means of an asymmetrically focusing incident-beam curved quartz monochromator. Measurements as a function of temperature were carried out using a liquid nitrogen 700 series Cryostream Cooler from Oxford Cryosystems. Cubic $Na_2Ca_3Al_2F_4$ was used for external calibration. The PEAKOC application from DIFFRACTINEL software was used for the calibration as well as for the peak

position determinations after pseudo-Voigt fittings and lattice parameters were refined by way of the least-squares option of the FullProf suite.[12, 13]

Specimens were introduced in a Lindemann capillary (0.5-mm diameter) and rotate perpendicularly to the X-ray beam during the experiments to improve the averaging of the crystallite orientations. Before each isothermal data acquisition, the specimen was allowed to equilibrate for about 10 min, and each acquisition time was no less than 1 h. The heating rate in-between data collection was 1.33 K min^{-1}. Patterns were recorded on heating in the temperature range from 100 K up to the melting point.

DIFFERENTIAL SCANNING CALORIMETRY (DSC)

Temperature (onset) and heat of fusion were obtained with a Q100 thermal analyzer from TA Instruments at a 10 K min^{-1} heating rate. The analyzer was calibrated using the melting point of indium (T_{fus} = 429.75 K and $\Delta_{fus}H$ = 28.45 J g^{-1}). The specimens were weighed using a microbalance sensitive to 0.01 mg and sealed in aluminum pans.

DENSITOMETRY OF THE MELT AS A FUNCTION OF TEMPERATURE

Liquid density as a function of temperature was measured with a DMA-5000 Density Meter from Anton-Paar. A melted specimen was introduced in the apparatus equilibrated at a temperature above the temperature of fusion. Data were obtained at isothermal steps while slowly cooling in the temperature range from 363 to 323 K. Dry air and bi-distilled water were used as calibration standards in the temperature range. The temperature was controlled at ±1 mK and measurements were performed when temperature fluctuations were smaller than ± 0.5 mK.

HIGH-PRESSURE DIFFERENTIAL THERMAL ANALYSIS (HP-DTA)

HP-DTA measurements have been carried out at a heating rate of 2 K min^{-1} using an in-house constructed high-pressure differential thermal analyzer similar to Würflinger's apparatus and operating in the 298 – 473 K and 0 – 250 MPa ranges.[14] To determine the melting temperature as a function of pressure and to ascertain that in-pan volumes were free from residual air, specimens were mixed with an inert perfluorinated liquid (Galden®, from Bioblock Scientics, Illkirch, France) as a pressure-transmitting medium, and the mixtures were sealed into cylindrical tin pans. To verify that the perfluorinated liquid was chemically inactive and did not interfere with the melting temperature of etifoxine, preliminary DSC measurements were carried out with a Galden®-etifoxine mixture on a Q100 analyzer of TA instruments without applied pressure.

RESULTS

CRYSTAL STRUCTURE

Racemic etifoxine was found to be monoclinic, space group P2$_1$/n (n°14), with unit-cell parameters a = 8.489(2) Å, b = 17.674(2) Å, c = 20.88(3) Å, β = 98.86(1)°, and V$_{cell}$ = 3095.8(9) Å^3 at 293 K containing Z = 8 molecules per unit-cell and Z' = 2 molecules in the asymmetric unit. The unit cell is in accordance with the unit-cell data published previously.[6, 7] Crystal- and structure-refinement data have been compiled in **Table 1** and non-H atom coordinates have been listed in **Table 2**. Other data (fractional coordinates for H-atoms, bond lengths, bond angles, anisotropic displacement parameters, and torsion angles) can be found in **Tables S1 to S5** of the **Supplementary Information**. The atom labelling is shown in **Figure 3**. The Cambridge Crystallographic Data Centre deposit (**CCDC** 1943706**)** contains the supplementary crystallographic data for this paper. It can be obtained free of charge from the CCDC via www.ccdc.cam.ac.uk/data_request/cif.

Table 1. Crystal- and structure-refinement data for racemic etifoxine[a]

Identification code / Empirical formula	etifoxine / $C_{17}H_{17}ClN_2O$
Formula weight	300.786 g mol^{-1}
Temperature	293(2) K
Wavelength	1.5418 Å
Crystal system (Space group)	Monoclinic (P 2_1/n)
Unit-cell dimensions	a = 8.489(2) Å, b = 17.674(2) Å, c = 20.883(3) Å, β = 98.860(10)°
Cell volume	3095.8(9) Å^3
Z, Z'	8, 2
Density (calculated)	1.291 g/cm^3
Absorption coefficient	2.178 mm^{-1}
F(000)	1264
Crystal size	0.550 x 0.200 x 0.100 mm^3
Theta range for data collection	3.292 to 64.944°.
Limiting indices	$0 \le h \le 9$, $0 \le k \le 20$, $-24 \le l \le 24$
Reflections collected / independent	5239 / 5239 [R(int) = 0.0162]
Completeness to theta = 64.944°	99.9 %
Absorption correction	Psi-scan
Max. and min. transmission	0.9971 and 0.8015
Refinement method	Full-matrix least-squares on F^2
Data / restraints / parameters	5239 / 0 / 382
Goodness-of-fit on F^2	1.131
Final R indices [I>2sigma(I)]	R1 = 0.0488, wR2 = 0.1272
R indices (all data)	R1 = 0.0589, wR2 = 0.1347
Extinction coefficient	0.0088(4)
Largest diff. peak and hole	0.3304 and -0.348 e.Å^{-3}

[a] esd's in parentheses

Table 2. Atom coordinates and equivalent isotropic displacement parameters U(eq) for racemic etifoxine[a]

Atom Identification[b]	x (× 10⁴)	y (× 10⁴)	z (× 10⁴)	U(eq)[c] (Å² × 10³)
Cl1_1	6465(1)	-3857(1)	-2(1)	70(1)
O1_1	10100(2)	-992(1)	1252(1)	46(1)
N1_1	7329(2)	-788(1)	1138(1)	43(1)
N2_1	9235(2)	147(1)	1445(1)	51(1)
C1_1	9944(2)	-1798(1)	1358(1)	45(1)
C2_1	8401(2)	-2046(1)	953(1)	42(1)
C3_1	7130(2)	-1531(1)	902(1)	40(1)
C4_1	8797(2)	-558(1)	1281(1)	42(1)
C5_1	8191(3)	-2753(1)	667(1)	50(1)
C6_1	6699(3)	-2964(1)	356(1)	51(1)
C7_1	5407(3)	-2484(1)	332(1)	51(1)
C8_1	5632(3)	-1769(1)	600(1)	48(1)
C9_1	9901(2)	-1946(1)	2075(1)	47(1)
C10_1	10259(3)	-1390(1)	2539(1)	60(1)
C11_1	10199(4)	-1536(2)	3183(1)	75(1)
C12_1	9808(4)	-2247(2)	3373(2)	85(1)
C13_1	9513(4)	-2808(2)	2921(2)	88(1)
C14_1	9546(4)	-2664(2)	2276(1)	71(1)
C15_1	8156(3)	784(1)	1421(1)	55(1)
C16_1	7782(5)	1125(2)	776(2)	105(1)
C17_1	11436(3)	-2134(2)	1149(1)	62(1)
Cl1_2	3065(1)	1044(1)	4949(1)	70(1)
O1_2	5459(2)	78(1)	2363(1)	48(1)
N1_2	2674(2)	253(1)	2174(1)	42(1)
N2_2	4203(3)	28(1)	1358(1)	53(1)
C1_2	5449(2)	-179(1)	3024(1)	44(1)
C2_2	4151(2)	258(1)	3282(1)	41(1)
C3_2	2779(2)	412(1)	2835(1)	39(1)
C4_2	4022(2)	113(1)	1975(1)	43(1)
C5_2	4233(3)	454(1)	3928(1)	46(1)
C6_2	2917(3)	780(1)	4137(1)	49(1)
C7_2	1525(3)	904(1)	3713(1)	50(1)
C8_2	1458(3)	724(1)	3069(1)	46(1)
C9_2	5090(3)	-1030(1)	3011(1)	46(1)
C10_2	5444(3)	-1480(2)	2514(1)	66(1)
C11_2	5062(4)	-2243(2)	2495(2)	79(1)
C12_2	4337(4)	-2561(2)	2976(2)	73(1)
C13_2	4047(4)	-2124(2)	3483(2)	73(1)
C14_2	4418(3)	-1361(1)	3501(1)	61(1)
C15_2	2978(3)	200(2)	807(1)	58(1)
C16_2	2579(4)	1026(2)	744(2)	81(1)
C17_2	7132(3)	-9(2)	3364(1)	58(1)

[a] esd's in parentheses

[b] The last digit of the atom numbering (1 or 2) corresponds to either of molecules 1 or 2, respectively.

[c] U(eq) is defined as one third of the trace of the orthogonalized U^{ij} tensor.
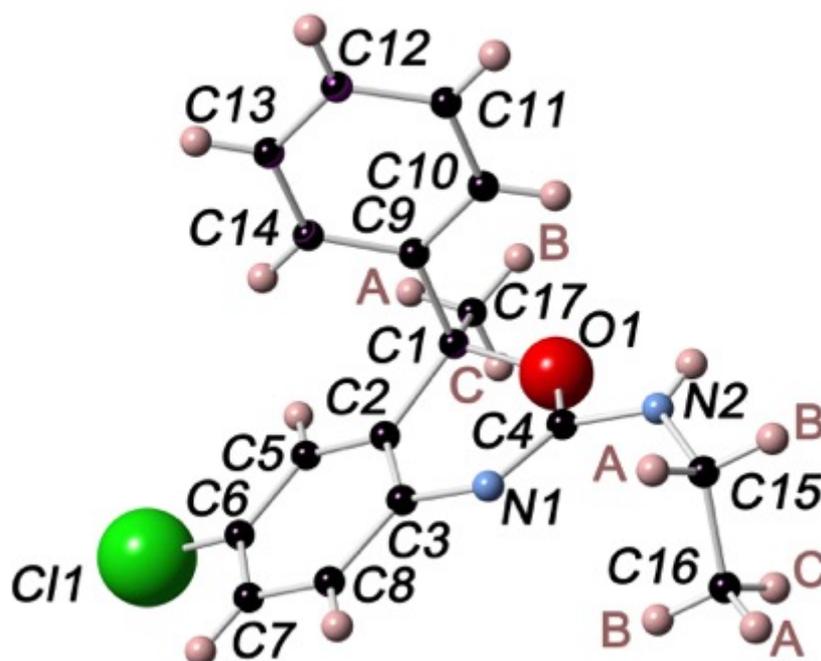
Figure 3. Molecular structure of R-etifoxine with atom identification. The hydrogen atoms are labelled with the same numbers as the atoms to which they are linked. When more than one H is linked to a C-atom, these H-atoms are labelled with supplementary letters A, B and C. The presented molecule is 2(*R*) in the racemate and the same labelling has been applied to molecule 1(*R*). The stereogenic center is atom C1.

THE SPECIFIC VOLUME OF RACEMIC ETIFOXINE AS A FUNCTION OF TEMPERATURE

An experimental and a calculated X-ray powder diffraction pattern are shown in **Figure S1** of the supplementary materials for comparison. It can be seen that the two patterns are virtually the same, although some differences in peak intensities indicate the presence of preferred orientation. High resolution X-ray diffraction patterns have been collected from 100 to 340 K to determine the lattice parameters of the unit cell as a function of temperature by least-squares refinement. The results have been compiled in **Table S6** in the supplementary materials. The specific volumes (v /cm^3 g^{-1}) have been fitted to the following quadratic equation as a function of temperature (T /K):

$$v_s = 0.74375(73) + 4.38(71){\times}10^{-5}\,T + 2.24(16){\times}10^{-7}\,T^2 \qquad (r^2{=}0.9995) \tag{1}$$

The specific volume of molten etifoxine from experimental density measurements have been reported in **Table S7** of the supplementary materials and have been fitted as a function of the temperature to the following equation:

$$v_{liq} = 0.6359(29) + 0.0006181(85)\,T \qquad (r^2 = 0.9993) \tag{2}$$

CALORIMETRIC BEHAVIOR

Specimens of the as-received sample were subjected to differential scanning calorimetry in closed pans. Heating from 213 K led to a single endothermic effect ascribed to a melting transition with a mean onset at 362.6 ±0.3 K. The mean value of the melting enthalpy was found to be 85.6 ±3.0 J g^{-1} (25.75 ±0.90 kJ mol^{-1}). On reheating after quick or slow cooling of the melt to 213 K, a midpoint glass transition was observed at 297.2 ±0.8 K. Data from 16 experiments have been compiled in **Table S8** of the supplementary materials. **Figure 4** contains typical DSC curves, one for the crystalline powder and one for the glass.
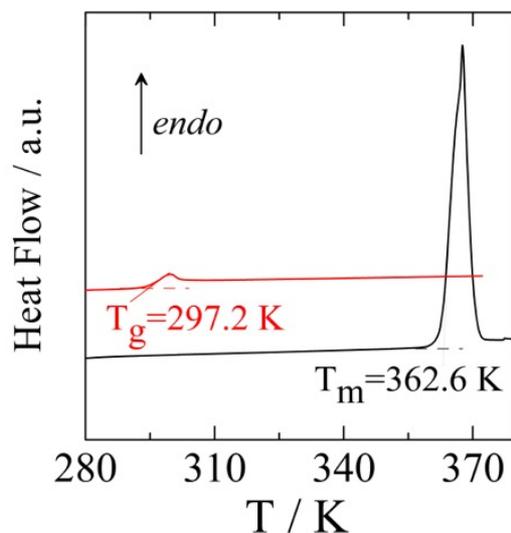
Figure 4. Differential scanning calorimetry curves of racemic monoclinic etifoxine obtained at 10 K min⁻¹. **(a)** First heating of the crystalline commercial product, T_m: melting temperature, **(b)** second heating after quenching the melt to 213 K in which a glass transition (T_g: glass transition temperature) can be observed.

THERMAL BEHAVIOR UNDER PRESSURE

A single endothermic peak of the fusion of racemic etifoxine was observed in the HP-DTA experiments. The onset temperature increases with the pressure presented in **Figure 5a** and the corresponding pressure-temperature phase diagram is depicted in **Figure 5b**. The onset temperatures (T /K) of the melting peaks and the corresponding pressures (P /MPa) listed in **Table S9** in the supplementary materials have been fitted to the quadratic equation:

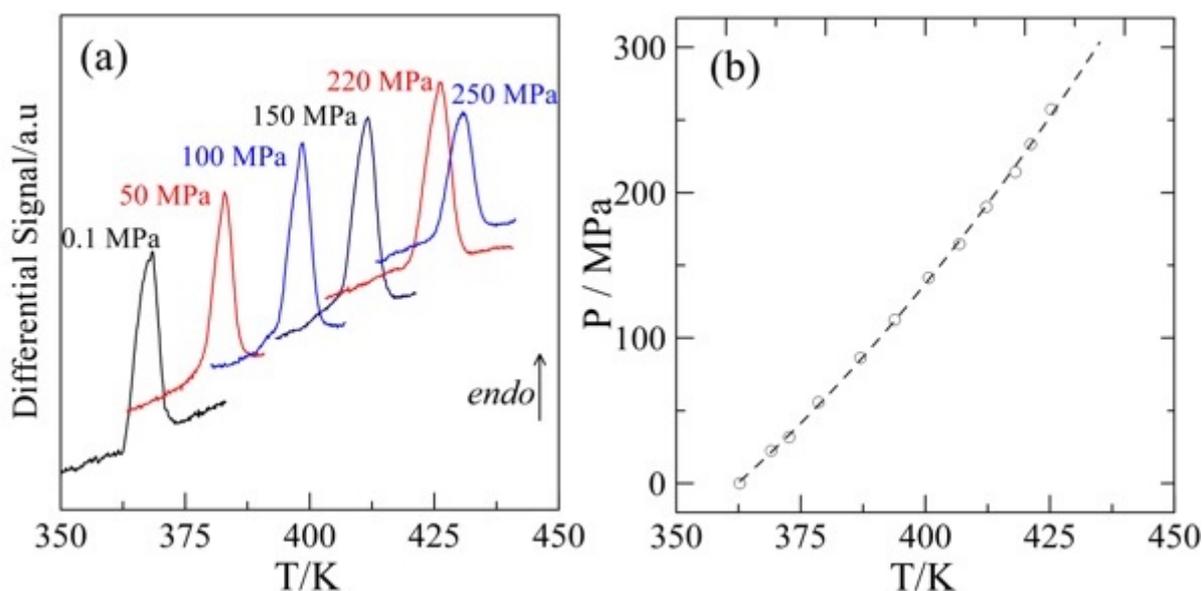$$P = 885(324) - 7.95(1.65)\,T + 0.0152(21)\,T^2 \qquad (r^2 = 0.9992) \qquad \textbf{(3)}$$

Figure 5. (a) Melting peaks of racemic etifoxine at various pressures and **(b)** the pressure-temperature phase diagram

DISCUSSION

CRYSTAL STRUCTURE

The centrosymmetric unit-cell of racemic etifoxine contains two independent molecules numbered 1 and 2 whose 3D projection is shown in **Figure 6**.
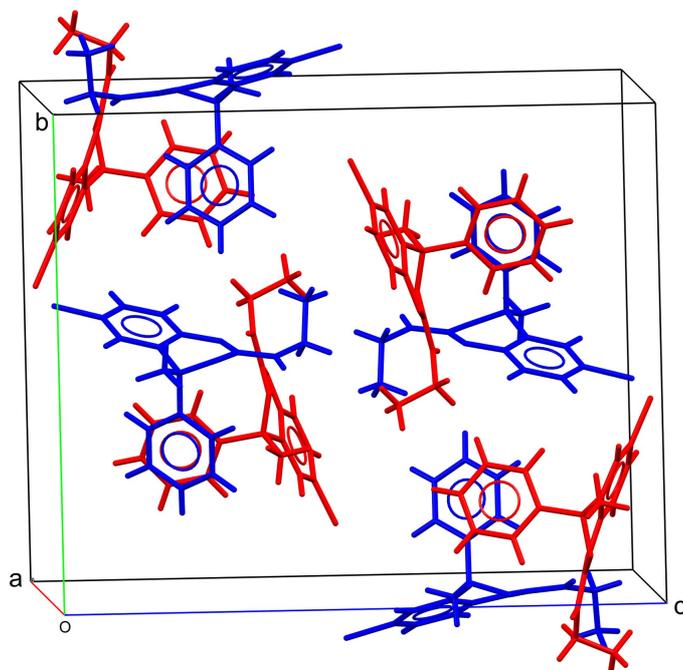

Figure 6. Monoclinic unit-cell of racemic etifoxine with the two independent molecules 1 (red) and 2 (blue).

The two independent molecules mainly differ in the orientations of the phenyl rings φ1 with respect to the heterocycles (see **Figure 7**): the values of the dihedral angles C2-C1-C9-C14 are 53.95° and -37.88° in molecules 1 and 2, respectively. Weak intramolecular interactions prevent the rotation of the two NH-CH$_2$-CH$_3$ chains around the N2-C4 bonds: N2-H2_1···O1_1 is 2.250 Å, and N2-H2_2···O1_2 equals 2.239 Å, as well as the rotation of the two phenyl rings φ1 around the C1-C9 bonds: C10-H10_1···O1_1 is 2.404 Å and C10-H10_2···O1_2 equals 2.454 Å. The molecules are held together by N1···H-N2 hydrogen bonds that form infinite chains parallel to the **a** axis and to the **ac** plane (see supplementary materials **Figure S2**). These interactions, in addition to the weak C-H···O interactions have been compiled in **Table S10** in the supplementary materials.
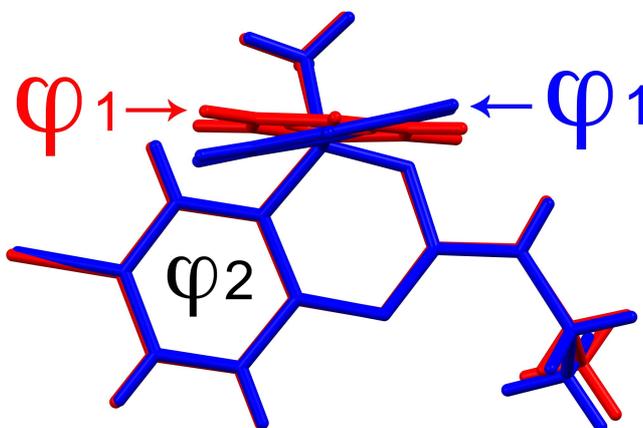

Figure 7. Superposition showing the difference in conformation of molecules 1 (red) and 2 (blue)

THERMAL EXPANSION OF THE SOLID AND THE LIQUID

Although the thermal expansion of the solid is best fitted by a quadratic equation (**eq. 1**), it can be approximated by a linear expression:

$$v_s(T) = 0.7343(11) + 0.0001426(46)\ T \qquad\qquad (r^2 = 0.9887) \qquad\qquad \textbf{(4)}.$$

An average expansivity of the solid $\alpha_{v,s}$ of 1.94×10^{-4} K^{-1} can be obtained by rewriting eq. 4 in the form of $v_s(T) = v_0 \times (1 + \alpha_{v,s}\ T)$. This solid expansivity is very close to the mean value for molecular organic solids of 2.21×10^{-4} K^{-1} that has been reported previously.[15-17]

The expansivity of liquid etifoxine is found to be 0.97×10^{-3} K^{-1} obtained from **eq. 2**. This is smaller than the mean value of $1.20 \pm 0.25 \times 10^{-3}$ K^{-1} found previously for the expansivity of molten active pharmaceutical ingredients;[16, 17] however, it still falls within the range of experimental uncertainty of 0.25×10^{-3} K^{-1}.

VOLUME CHANGE ON MELTING AND VOLUME DIFFERENCE AT THE GLASS TRANSITION

It has been previously reported that, in the case of molecular organic solids, the change in the specific volume on melting is about 11 ± 3 %,[16-18] i.e. slightly smaller than the 12 % value found previously by Goodman et al.[19] Calculating the specific volumes of the solid and of the liquid using **eqs. 1 and 2** at $T_{fus} = 362.6$ K, it is found that the volume change on melting is in the present case 0.0709 cm^3 g^{-1}, leading to the value of 1.090 ± 0.010 for the v_{liq}/v_s ratio at T_{fus}, in fair agreement with the above-mentioned value.

At the glass transition, the metastable undercooled melt rigidifies, *i.e.* becomes as viscous as the crystalline solid. The glass transition temperature has been found at 297.2 K (10 K min^{-1}). The specific volume of the melt at T_g can be calculated with **eq. 2** and is found to be 0.8196 cm^3 g^{-1}, while that of the crystalline solid at this temperature is 0.7766 cm^3 g^{-1} from eq. 1. Thus, the ratio v_{glass}/v_s at T_g equals 1.055 ± 0.010, *i.e.* the volume difference between the crystalline and the amorphous phase is approximately half that of the difference at the melting point. With this information, one can draw the temperature - (specific) volume diagram, shown in **Figure 8**, which is a partial projection of $F(v,T)$, the Helmholtz function of the system, on a T-v plane, one of the four thermodynamically equivalent energy functions of the system. v_{glass}/v_s ratios have been found for other cases, which have been compiled in **Table 3**.
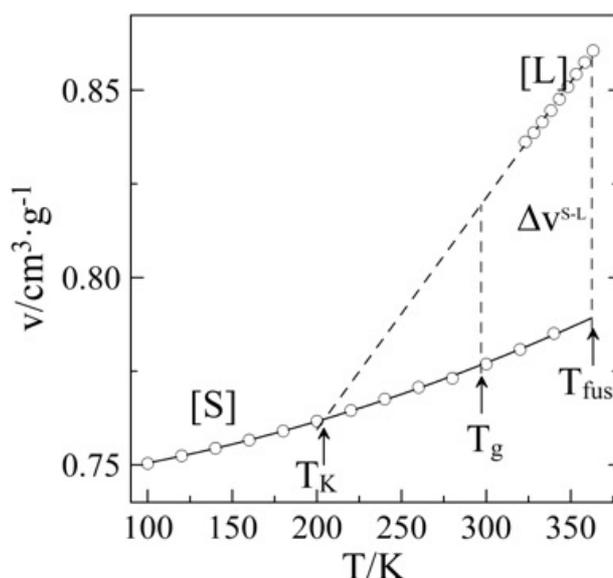

Figure 8. Specific volumes of solid (S) and liquid (L) etifoxine as a function of temperature with extrapolation to the Kauzmann temperature $T_k = 204.6$ K using eqs. 1 and 2.

Table 3. Experimental volume changes for molecular compounds and pharmaceuticals at their melting point and glass transition temperature

compound	v_L/v_l at T_{fus}	T_{fus}/K	v_L/v_l at T_g	T_g /K	T_g/T_{fus}	Reference
paracetamol	1.15	442.3	1.07	298	0.673	[20]
prilocaine	1.13	311.5	1.07	218	0.700	[21]
rimonabant	1.11	429.2	1.04	350	0.820	[22]
biclotymol	1.13	400.5	1.05	294	0.734	[23]
ternidazole	1.11	333.0	1.07	235	0.706	[24]
morniflumate	1.12	348.1	1.06	249	0.715	[18]
etifoxine	1.09	362.4	1.055	297.2	0.820	This work
Mean	1.12(2)		1.06(1)			

SLOPE OF THE SOLID-LIQUID EQUILIBRIUM IN THE PRESSURE-TEMPERATURE DIAGRAM

Using **eq. 3**, it is found that the slope of the melting equilibrium of racemic etifoxine at P = 0 MPa equals 3.29 ±0.06 MPa K^{-1} (Figure 5b). This slope can also be determined through the Clapeyron equation dP/dT = $\Delta_{fus}H/(T_{fus} \Delta v)$ in which $\Delta_{fus}H$ is the melting enthalpy (85.60 J g^{-1}), T_{fus} the melting temperature (362.6 K), and Δv the volume change on melting (0.07094 cm^3 g^{-1}). With these experimental values, the value of dP/dT is found to be 3.33 ±0.12 MPa K^{-1}, i.e. extremely close to the direct experimental value of 3.29 MPa K^{-1}, indicating that at least in the case of etifoxine, the Clapeyron equation is a good alternative for direct measurements to obtain the response of the system to pressure.

ISOBARIC THERMAL EXPANSION TENSOR FOR THE SOLID

The anisotropy of the intermolecular interactions can be accounted for by the isobaric thermal expansion tensor, which shows the influence of these interactions in the crystal on heating.[25] The eigenvalues and the eigenvectors of the tensor specify the strongest and the weakest directions for the intermolecular interactions, commonly referred to as "hard" and "soft" directions, respectively.[25]

The lattice parameters as a function of temperature have been determined (see supplementary materials, **Table S6**) and fitted using the least-squares method. The coefficients of the related polynomial equations have been compiled in **Table S11** in the supplementary materials, together with the reliability factor, defined as $R=\Sigma(y_{oi} - y_{ci})^2/y_{ci}^2$, where y_{oi} and y_{ci} are the measured and calculated lattice constants, respectively.

The procedure to determine the eigenvalues and eigenvectors of the second-rank α_{ij} thermal expansion tensor has been detailed previously.[25] For monoclinic symmetry, the tensor is fully defined by three eigenvalues α_i (i = 1,2,3) and by an angle between the direction of one of the eigenvectors (α_1 in the present case) and the crystallographic axis *a*, the α_2 direction being parallel to the two-fold axis *b*. **Figure 9** depicts the variation of the eigenvalues of the thermal-expansion tensor as a function of temperature as well as the 3D-tensor within the orthogonal frame of eigenvectors together with the crystallographic axes at 140 K. The tensor is rather anisotropic and this anisotropy increases with temperature. The thermal expansion within the *ab* plane is the highest ("soft" plane) while the lowest deformation (α_3 direction) corresponding to a "hard direction" is found within the *ac* plane as a consequence of the intermolecular hydrogen bonding (N2-H···N1).
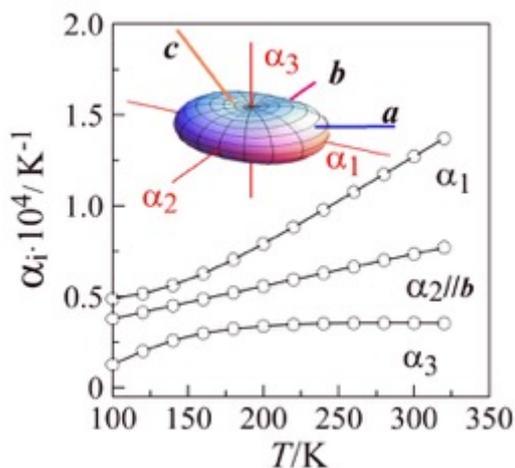
Figure 9. α_i eigenvalues of the thermal-expansion tensor as a function of temperature for the P2$_1$/n monoclinic phase of etifoxine with the $\pmb{\alpha_2}$ eigenvector parallel to the two-fold crystallographic axis $\pmb{b}$, as evidenced in the tensor representation at 140 K in the inset (full length scale of the α_i eigenvectors corresponds to 10^{-4} K^{-1}).

CONCLUDING REMARKS

The crystal structure of racemic etifoxine has been solved at room temperature and thermal expansion studies in the range from 100 K to 340 K as well as differential scanning calorimetry did not reveal any crystalline polymorphism. However the crystal structure contains two independent molecules (Z' = 2) with different conformations, which implies a possibility for etifoxine to exhibit conformational polymorphism as previously defined by Bernstein and Hagler.[26]

It has been shown that the thermal expansion of etifoxine is very similar to that of small organic molecules in general, for the solid as well as for the liquid. As far as the volume change on melting is concerned, it has been found that, again in the present case, it agrees with the average value of 11% within an error of less than 3%. In addition, the volume difference between the crystal and the metastable liquid at the temperature of the glass transition is found to be about 6 %, in close accordance with previously found data. Further case studies are still needed before one can conclude that these volume changes for molecular organic compounds are more or less independent of the chemical composition and thus 'statistically' and possibly in a deeper sense universal.

REFERENCES

1.   Kuch, H.; Seidl, G.; Hoffmann, I.; Soden, B. 3,1-benzothiazines and 3,1-benzoxazines. 1968.
2.   Choi, Y. M.; Kim, K. H., Etifoxine for Pain Patients with Anxiety. *Korean J. Pain* **2015,** *28* (1), 4-10.
3.   Besnier, N.; Blin, O., Étifoxine: études cliniques récentes. *L'encéphale* **2008,** *34 (suppl 1)*, S9-S14.
4.   Girard, C.; Liu, S.; F., C.; Adams, D.; Lacroix, C.; Verleye, M.; Gillardin, J. M.; Baulieu, E.-E.; Schumacher, M.; Schweizer-Groyer, G., Etifoxine improves peripheral nerve regeneration and functional recovery. *PNAS* **2008,** *105* (51), 20505-20510.
5.   Nguyen, N.; Fakra, E.; Pradel, V.; Jouve, E.; Alquier, C.; Le Guern, M.-E.; Micallef, J.; Blin, O., Efficacy of etifoxine compared to lorazepam monotherapy in the treatment of

patients with adjustment disorders with anxiety: a double-blind controlled study in general practice. *Hum. Psychopharmacol. Clin. Exp.* **2006,** *21*, 139-149.

6.   Paulus, E. F.; Bartl, H.; Ruggeberg, K., CSD entry ECMPBX. *Eur. Cryst. Meeting* **1976**, 442.

7.   Paulus, E. F.; Bartl, H.; Ruggeberg, K., CSD Entry ECMPBX01. *Eur. Cryst. Meeting* **1976**, 442.

8.   Enraf-Nonius *CAD4 Express Software*, Enraf Nonius: Delft, The Netherlands, 1994.

9.   Harms, K.; Wocadlo, S. *XCAD-CAD4 Data reduction*, University of Marburg: Marburg, 1995.

10.   Sheldrick, G. M. *SHELXL97: Program for crystal structure refinement*, Universität Göttingen: Göttingen, Germany, 1997.

11.   Sheldrick, G. M., A short history of SHELX. *Acta Crystallogr. A* **2008,** *64*, 112-122.

12.   Rodriguez-Carvajal, J., Recent advances in magnetic structure determination by neutron powder diffraction. *Physica B* **1993,** *192*, 55-69.

13.   Rodriguez-Carvajal, J.; Roisnel, T.; Gonzales-Platas, J. *Full-Prof suite version 2005*, Laboratoire Léon Brillouin, CEA-CNRS, CEN Saclay, France, 2005.

14.   Würflinger, A., Differential thermal-analysis under high-pressure IV. Low-temperature DTA of solid-solid and solid-liquid transitions of several hydrocarbons up to 3 kbar. *Ber. Bunsen-Ges. Phys. Chem.* **1975,** *79* (12), 1195-1201.

15.   Gavezzotti, A., *Molecular Aggregation. Structure Analysis and Molecular Simulation of Crystals and Liquids*. Oxford University Press: Oxford, UK, 2013; p 448.

16.   Céolin, R.; Rietveld, I. B., The topological pressure-temperature phase diagram of ritonavir, an extraordinary case of crystalline dimorphism. *Ann. Pharm. Fr.* **2015,** *73* (1), 22-30.

17.   Rietveld, I. B.; Céolin, R., Phenomenology of crystalline polymorphism: overal monotropic behavior of the cardiotonic agent FK664 forms A and B. *J. Therm. Anal. Calorim.* **2015,** *120* (2), 1079-1087.

18.   Barrio, M.; Tamarit, J. L.; Ceolin, R.; Robert, B.; Guechot, C.; Teulon, J. M.; Rietveld, I. B., Experimental and topological determination of the pressure temperature phase diagram of morniflumate, a pharmaceutical ingredient with anti-inflammatory properties. *J. Chem. Thermodyn.* **2017,** *112*, 308-313.

19.   Goodman, B. T.; Wilding, W. V.; Oscarson, J. L.; Rowley, R. L., A note on the relationship between organic solid density and liquid density at the triple point. *J. Chem. Eng. Data* **2004,** *49* (6), 1512-1514.

20.   Espeau, P.; Céolin, R.; Tamarit, J. L.; Perrin, M. A.; Gauchi, J. P.; Leveiller, F., Polymorphism of paracetamol: Relative stabilities of the monoclinic and orthorhombic phases inferred from topological pressure-temperature and temperature-volume phase diagrams. *J. Pharm. Sci.* **2005,** *94* (3), 524-539.

21.   Rietveld, I. B.; Perrin, M.-A.; Toscani, S.; Barrio, M.; Nicolaï, B.; Tamarit, J.-L.; Céolin, R., Liquid-Liquid Miscibility Gaps in Drug-Water Binary Systems: Crystal Structure and Thermodynamic Properties of Prilocaine and the Temperature-Composition Phase Diagram of the Prilocaine-Water System. *Mol. Pharmaceut.* **2013,** *10* (4), 1332-1339.

22.   Perrin, M. A.; Bauer, M.; Barrio, M.; Tamarit, J. L.; Ceolin, R.; Rietveld, I. B., Rimonabant dimorphism and its pressure-temperature phase diagram: a delicate case of overall monotropic behavior. *J. Pharm. Sci.* **2013,** *102* (7), 2311-21.

23.   Ceolin, R.; Tamarit, J. L.; Barrio, M.; Lopez, D. O.; Nicolai, B.; Veglio, N.; Perrin, M. A.; Espeau, P., Overall monotropic behavior of a metastable phase of biclotymol, 2,2'-methylenebis(4-chloro-3-methyl-isopropylphenol), inferred from experimental and

topological construction of the related P-T state diagram. *J. Pharm. Sci.* **2008,** *97* (9), 3927-41.

24.   Mahé, N.; Perrin, M.; Barrio, M.; Nicolaï, B.; Rietveld, I.; Tamarit, J.; Céolin, R., Solid-State Studies of the Triclinic (Z '=2) Antiprotozoal Drug Ternidazole. *J. Pharm. Sci.* **2011,** *100* (6), 2258-2266.

25.   Salud, J.; Barrio, M.; Lopez, D. O.; Tamarit, J. L.; Alcobe, X., Anisotropy of intermolecular interactions from the study of the thermal-expansion tensor. *J. Appl. Crystallogr.* **1998,** *31*, 748-757.

26.   Bernstein, J.; Hagler, A. T., Conformational polymorphism. The influence of crystal-structure on molecular-conformation. *J. Am. Chem. Soc.* **1978,** *100* (3), 673-681.